

Bremsstrahlung simulation in $K \rightarrow \pi l^\pm \nu_l(\gamma)$ decays

Qingjun Xu^{a,b} and Z. Was^{b,c}

^a *Department of Physics, Hangzhou Normal University, Hangzhou 310036, China*

^b *Institute of Nuclear Physics, PAN, Kraków, ul. Radzikowskiego 152, Poland*

^c *CERN PH-TH, CH-1211 Geneva 23, Switzerland*

ABSTRACT

In physics simulation chains, the PHOTOS Monte Carlo program is often used to simulate QED effects in decays of intermediate particles and resonances.

The program is based on an exact multiphoton phase space. In general, the matrix element is obtained from iterations of a universal kernel and approximations are involved. To evaluate the program precision, it is necessary to formulate and implement within the generator the exact matrix element, which depends on the decay channel. Then, all terms necessary for non-leading logarithms are taken into account. In the present letter we focus on the decay $K \rightarrow \pi l^\pm \nu_l$ and tests of the PHOTOS Monte Carlo program. We conclude a 0.2% relative precision in the implementation of the hard photon matrix element into the emission kernel, including the case where approximations are used.

Submitted to Eur. Phys. J. C

IFJPAN-IV-2011-14
CERN-PH-TH/2011-309
December, 2011

[†] Work of ZW is supported in part by the Polish Ministry of Science and Higher Education grant No. 1289/B/H03/2009/37., Q. Xu is supported by China-Poland inter-governmental cooperation grant 34-13, National Natural Science Foundation of China under Grant No. 11147023 and Zhenjiang Provincial Natural Science Foundation of China under Grant No. LQ12A05003.

1 Introduction

Semileptonic flavour changing decays, such as $K \rightarrow \pi l^\pm \nu_l$ offer a window for measurements of Standard Model basic couplings: quark mixing angles [1]. Moreover properties of low and medium energy hadronic interactions manifest themselves in such decays. It is thus important to keep control of decay products distributions in a form suitable for comparisons with data and without losing control of the underlying quark level matrix element.

Comparison between experimental data and theoretical predictions relies on Monte Carlo simulation to take into account the detector response [2]. Given today's experimental precision, generators used in such comparisons must be based on exact phase space and explicit formulation of the matrix element. Otherwise the discussion of theoretical uncertainties in realistic applications is rather difficult.

QED bremsstrahlung must be taken into account in these comparisons too. Infrared singularities cancel out in sufficiently inclusive observables. In a first approximation, the QED bremsstrahlung amplitude can be factorized as the Born amplitude and an emission (eikonal or collinear) term. This can be done for a calculation at a fixed order of perturbation expansion, but it holds to all orders and is known under the name of exponentiation [3] (for application in Monte Carlo simulation see e.g. [4, 5]). In phase space regions where photons are collinear to charged particles, factorization theorems define the dominant terms of the amplitudes. This is why, bremsstrahlung can be treated to a good precision independently of the decay channel. As a consequence predictions, which neglect QED effects, represent a valid segment of the phenomenology work.

For the decays of a given particle, matrix elements based Monte Carlo generators are prepared either by theorists working on effective lagrangians (also on QCD based predictions), or by experimental physicists. Since many years the PHOTOS Monte Carlo program [6, 7] is used for simulation of bremsstrahlung in decays. It represents a separate segment of the simulation chain.

With the increased precision of new available data, such an implementation requires a careful discussion of its systematic errors, which has to be repeated for each decay mode. The phenomenological importance of approximations needs to be analyzed, and the factorization of QED emission terms need to be reviewed, using as a reference solutions based on exact phase space and matrix element for the whole decay (thus including QED bremsstrahlung).

The PHOTOS Monte Carlo program was presented for the first time in Ref. [6]. The universal kernel was introduced and was shown to work, within expected accuracy, in cases where comparisons with first order matrix element reference simulation programs were available. In references [7] and [8] the notion of iteration was introduced in the PHOTOS program, first, for double photon emission, and later for multiple photon emission. Because of a rather unique order of iteration (iteration over sources providing collinear singularities is performed first, then construction of consecutive photon is started), the algorithm is compatible at the same time with an exclusive exponentiation and resummation of collinear logarithms.

In reference [9] a discussion of the exact matrix element implemented within the PHOTOS

kernel was performed for the Z decay. The discussion was continued in Ref. [10] for the decay of a scalar into pair of scalars. In this study, a detailed presentation of the phase space parametrization was given and it was followed in [11] by a discussion of the matrix elements of the W leptonic decay and the decay of virtual photons to pairs of scalars. Matrix element weights became available for public use with [12].

Until now, discussions of matrix elements were addressing two-body decays only. In this case, not only phase space at Born level is particularly simple, but also photon emission is easy to handle.

In the present work, we focus on the K_{l3} decay for which a three-body kinematic is present already at the Born level. By studying this decay, we test not only the matrix element implementation effects, but also the PHOTOS phase space generation¹.

Our study is organized as follows. In Section 2 we present the matrix elements for K_{l3} decays, at Born level and in the case of single photon emission. Results of calculations based on scalar QED [13] and on ChPT [14, 15, 16] with truncations as in Refs. [17, 18] are compared and discussed. In this context we also investigate matrix elements and their factorization properties. In Section 3, we consider fully differential distributions. For that purpose squared matrix element are reviewed and possible options resulting from physics assumptions (scalar QED or [17, 18]) are shown. We address again factorization properties, this time stressing features which are useful when constructing a Monte Carlo program. The set-up and implementations prepared for tests are presented in Section 4. Numerical results are collected in Section 5. Conclusions, including an estimate of PHOTOS Monte Carlo simulation precision for K_{l3} decays, are given in Section 6.

2 Amplitudes for $K_{e3}(\gamma)$ decays.

In the first sub-section we present the amplitude for the decay of charged kaons. In the second one the case of the neutral kaon is considered, similarities of the two cases are investigated as well.

2.1 Amplitude for $K^-(p) \rightarrow \pi^0(q) + e^-(p_e) + \bar{\nu}_e(p_\nu)$ decay

Let us start the discussion from the amplitude of the decay

$$K^-(p) \rightarrow \pi^0(q) + e^-(p_e) + \bar{\nu}_e(p_\nu) \quad (1)$$

¹Parametrization of phase space in PHOTOS is explicit and exact, if the presampler for collinear emissions is used only along a single charge. Otherwise, starting from the moment when the photon is supposed to be added to a more than two-body configuration, an approximation appears when the phase space Jacobians for the multitude of branches are combined. This can be improved, but for test cases with second order matrix elements in Z decay [9], we have found that this approximation is necessary, unless complete double photon emission amplitude would be installed into the program at the same time.

taken at the Born level. With the notation of Ref. [17, 18] it reads

$$M_{\text{Born}}^c = \frac{e^2 V_{us} F_{K\pi}(t) (p+q)^\mu}{8\sqrt{2} s_W^2 (t - M_W^2)} \bar{u}(p_e, \lambda_e) \gamma_\mu (1 - \gamma_5) v(p_\nu, \lambda_\nu), \quad (2)$$

where $\lambda_e(\lambda_\nu)$ denote the electron (neutrino) helicity, $F_{K\pi}(t)$ is the form factor and $t = (p - q)^2$. Because of the relatively small mass of the K meson, t is always $\ll M_W^2$ and the amplitude simplifies to

$$M_{\text{Born}}^c = \frac{G_F V_{us} F_{K\pi}(t)}{2} (p+q)^\mu \bar{u}(p_e, \lambda_e) \gamma_\mu (1 - \gamma_5) v(p_\nu, \lambda_\nu). \quad (3)$$

Let us now consider the amplitudes for single photon emission. We follow Ref. [11] and

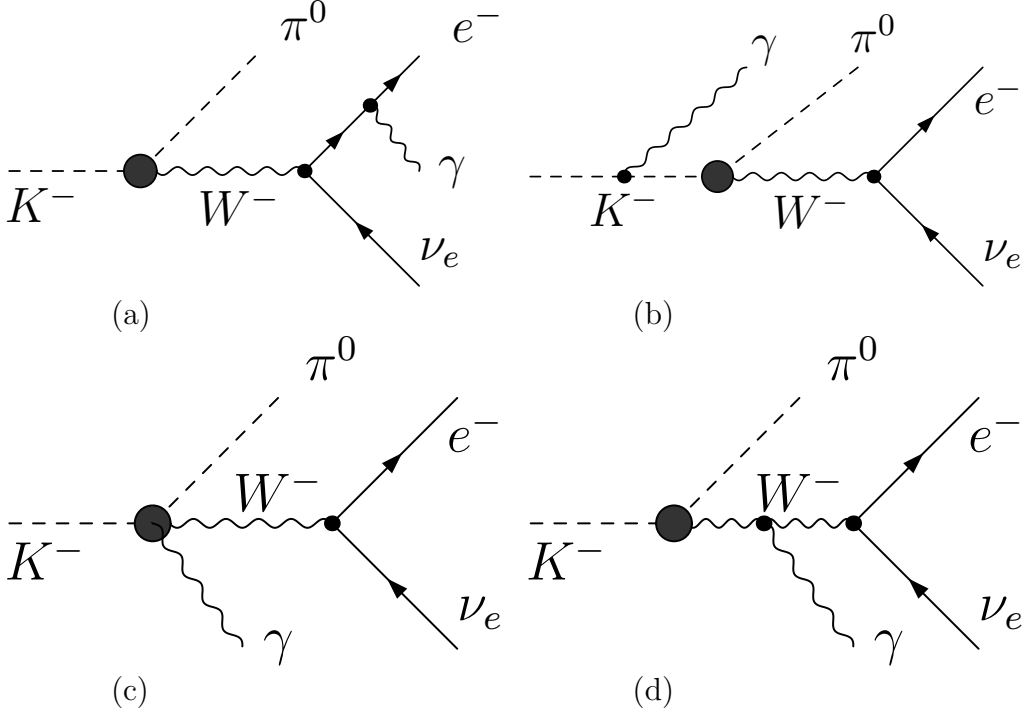


Figure 1: Feynman diagrams of the $K^- \rightarrow \pi^0 e^- \bar{\nu}_e \gamma$ decay.

we define the photon polarization states in the rest frame of the K meson. This choice fixes the gauge. However, our amplitudes are expressed in a Lorentz and gauge invariant formulation.

Scalar QED diagrams for $K^-(p) \rightarrow \pi^0(q) e^-(p_e) \bar{\nu}_e(p_\nu) \gamma(k)$ decay are presented in Figure 1. The contribution of diagram (d) is proportional to $1/M_W^4$ while for other diagrams it is proportional to $1/M_W^2$. For this reason, we can neglect the contribution of (d). The

amplitude of the $K^- \rightarrow \pi^0 e^- \bar{\nu}_e \gamma$ decay reads:

$$\begin{aligned}
M^c &= \frac{G_F V_{us} F_{K\pi}(t)}{2} \bar{u}(p_e, \lambda_e) [Q_e (p+q)^\mu \\
&\quad \left(\frac{p_e \cdot \epsilon}{p_e \cdot k} + \frac{\not{\epsilon} \not{k}}{2 p_e \cdot k} \right) - Q_K (p+q-k)^\mu \frac{p \cdot \epsilon}{p \cdot k} \\
&\quad - Q_K \epsilon^\mu] \gamma_\mu (1 - \gamma_5) v(p_\nu, \lambda_\nu), \tag{4}
\end{aligned}$$

where Q_e, Q_K denote the charges of e^- and K^- respectively. To visualize its factorization properties this amplitude can be expressed as a sum of three gauge invariant terms:

$$M^c = M_I^c + M_{II}^c + M_{III}^c, \tag{5}$$

where

$$\begin{aligned}
M_I^c &= \frac{G_F V_{us} F_{K\pi}(t)}{2} (p+q)^\mu \left(Q_e \frac{p_e \cdot \epsilon}{p_e \cdot k} - Q_K \frac{p \cdot \epsilon}{p \cdot k} \right) \\
&\quad \bar{u}(p_e, \lambda_e) \gamma_\mu (1 - \gamma_5) v(p_\nu, \lambda_\nu), \tag{6}
\end{aligned}$$

$$\begin{aligned}
M_{II}^c &= \frac{G_F V_{us} F_{K\pi}(t)}{2} (p+q)^\mu \bar{u}(p_e, \lambda_e) Q_e \frac{\not{\epsilon} \not{k}}{2 p_e \cdot k} \\
&\quad \gamma_\mu (1 - \gamma_5) v(p_\nu, \lambda_\nu), \tag{7}
\end{aligned}$$

$$\begin{aligned}
M_{III}^c &= \frac{G_F V_{us} F_{K\pi}(t)}{2} Q_K \left(k^\mu \frac{p \cdot \epsilon}{p \cdot k} - \epsilon^\mu \right) \\
&\quad \bar{u}(p_e, \lambda_e) \gamma_\mu (1 - \gamma_5) v(p_\nu, \lambda_\nu). \tag{8}
\end{aligned}$$

The first term M_I^c consists of the Born-level amplitude times an eikonal factor. The second, M_{II}^c , is free of soft singularity but contributes logarithmically in the collinear limit. Finally the third term, M_{III}^c , is free of both soft and collinear singularities. Hence, formula (5) provides a clearly structured expression of the amplitude.

For each term (6,7,8) a separation into leptonic and hadronic parts is visible. It is encouraging, because it coincides with the structure which was useful in [11]. In our present work we again see that the first two parts are process independent in their emission aspect, and only the last non-dominant part breaks this property². This is why, we expect this formulation to be useful for our numerical discussion.

To prepare a comparison with amplitudes of Ref. [17] the Born and photon emission amplitudes (equations (3) and (4)), can be written thanks to Dirac equation as:

$$\begin{aligned}
M_{\text{Born}}^c &= \frac{G_F V_{us} F_{K\pi}(t)}{2} \\
&\quad \bar{u}(p_e, \lambda_e) (2 \not{q} + m_e) (1 - \gamma_5) v(p_\nu, \lambda_\nu) \tag{9}
\end{aligned}$$

²Expression (8) coincides also with the similar term (19) discussed later in the amplitude of the $K^0 \rightarrow \pi^\mp l^\pm \nu_l$ decay.

and

$$\begin{aligned}
M^c = & \frac{G_F V_{us} F_{K\pi}(t)}{2} \bar{u}(p_e, \lambda_e) \left[\left(Q_e \frac{p_e \cdot \epsilon}{p_e \cdot k} - Q_K \frac{p \cdot \epsilon}{p \cdot k} \right) \right. \\
& \left. + Q_e \frac{\not{\epsilon} \not{k}}{2 p_e \cdot k} \right] (2 \not{q} + m_e) (1 - \gamma_5) v(p_\nu, \lambda_\nu).
\end{aligned} \tag{10}$$

This new formulation coincides with formula (13) of Ref. [17]. In that paper, the form factor is taken at $t = 0$ (see there, formulae (2) and (3)), we follow the same choice.

The new form of the amplitude can also be splitted into two gauge invariant parts:

$$M^c = M_{I'}^c + M_{II'}^c \tag{11}$$

where

$$\begin{aligned}
M_{I'}^c = & \frac{G_F V_{us} F_{K\pi}(t)}{2} \bar{u}(p_e, \lambda_e) \left(Q_e \frac{p_e \cdot \epsilon}{p_e \cdot k} - Q_K \frac{p \cdot \epsilon}{p \cdot k} \right) \\
& (2 \not{q} + m_e) (1 - \gamma_5) v(p_\nu, \lambda_\nu),
\end{aligned} \tag{12}$$

$$\begin{aligned}
M_{II'}^c = & \frac{G_F V_{us} F_{K\pi}(t)}{2} \bar{u}(p_e, \lambda_e) Q_e \frac{\not{\epsilon} \not{k}}{2 p_e \cdot k} \\
& (2 \not{q} + m_e) (1 - \gamma_5) v(p_\nu, \lambda_\nu).
\end{aligned} \tag{13}$$

The first gauge invariant part has the form of a born-like amplitude times an eikonal factor. The second one does not contribute to soft singularities, but contribute to collinear singularities. Unfortunately formulae (12, 13) do not manifest the process independent form which is useful for construction of Monte Carlo programs.

For all amplitudes presented above as well as their parts, the terms proportional to the electron mass were carefully kept. The results naturally extend to the case of the $K^- \rightarrow \pi^0 \mu^- \bar{\nu}_\mu$ decay.

2.2 Amplitude for $K^0(p) \rightarrow \pi^+(q) + e^-(p_e) + \bar{\nu}_e(p_\nu)$ decay

The $K^0(p) \rightarrow \pi^+(q) + e^-(p_e) + \bar{\nu}_e(p_\nu)$ decay is interesting from the point of view of Monte Carlo discussions, even though in this case effects of bremsstrahlung are of lesser phenomenological relevance. There are not only two charged particles of different masses in the final state, but there is also a spectator $\bar{\nu}_e$, important from the point of view of phase space generation.

The charged and neutral K decays amplitudes are quite similar. The Born level amplitude reads:

$$\begin{aligned}
M_{\text{Born}}^0 = & \frac{G_F V_{us} F_{K\pi}(t)}{\sqrt{2}} (p + q)^\mu \\
& \bar{u}(p_e, \lambda_e) \gamma_\mu (1 - \gamma_5) v(p_\nu, \lambda_\nu).
\end{aligned} \tag{14}$$

The amplitude for single photon emission is again quite short

$$\begin{aligned}
M^0 &= \frac{G_F V_{us} F_{K\pi}(t)}{\sqrt{2}} \bar{u}(p_e, \lambda_e) [Q_e (p+q)^\mu \\
&\quad \left(\frac{p_e \cdot \epsilon}{p_e \cdot k} + \frac{\not{\epsilon} \not{k}}{2p_e \cdot k} \right) + Q_\pi (p+q+k)^\mu \frac{q \cdot \epsilon}{q \cdot k} \\
&\quad - Q_\pi \epsilon^\mu] \gamma_\mu (1 - \gamma_5) v(p_\nu, \lambda_\nu)
\end{aligned} \tag{15}$$

and can be expressed as a sum of three gauge invariant parts:

$$M^0 = M_I^0 + M_{II}^0 + M_{III}^0, \tag{16}$$

where

$$\begin{aligned}
M_I^0 &= \frac{G_F V_{us} F_{K\pi}(t)}{\sqrt{2}} (p+q)^\mu \left(Q_e \frac{p_e \cdot \epsilon}{p_e \cdot k} + Q_\pi \frac{q \cdot \epsilon}{q \cdot k} \right) \\
&\quad \bar{u}(p_e, \lambda_e) \gamma_\mu (1 - \gamma_5) v(p_\nu, \lambda_\nu),
\end{aligned} \tag{17}$$

$$\begin{aligned}
M_{II}^0 &= \frac{G_F V_{us} F_{K\pi}(t)}{\sqrt{2}} (p+q)^\mu \bar{u}(p_e, \lambda_e) Q_e \frac{\not{\epsilon} \not{k}}{2p_e \cdot k} \\
&\quad \gamma_\mu (1 - \gamma_5) v(p_\nu, \lambda_\nu),
\end{aligned} \tag{18}$$

$$\begin{aligned}
M_{III}^0 &= \frac{G_F V_{us} F_{K\pi}(t)}{\sqrt{2}} Q_\pi \left(k^\mu \frac{q \cdot \epsilon}{q \cdot k} - \epsilon^\mu \right) \\
&\quad \bar{u}(p_e, \lambda_e) \gamma_\mu (1 - \gamma_5) v(p_\nu, \lambda_\nu).
\end{aligned} \tag{19}$$

Here Q_π denotes the π^\pm charge. As in the case of K^\pm , only the first part (formula (17)) is infrared singular, and the third part is free of collinear singularity.

With the help of the Dirac equation we can transform (15) into:

$$\begin{aligned}
M^0 &= \frac{G_F V_{us} F_{K\pi}(t)}{\sqrt{2}} \bar{u}(p_e, \lambda_e) \left[\left(Q_e \frac{p_e \cdot \epsilon}{p_e \cdot k} + Q_\pi \frac{q \cdot \epsilon}{q \cdot k} \right) \right. \\
&\quad \left. + Q_e \frac{\not{\epsilon} \not{k}}{2p_e \cdot k} \right] (2 \not{q} + m_e) (1 - \gamma_5) v(p_\nu, \lambda_\nu) \\
&\quad + 2 \frac{G_F V_{us} F_{K\pi}(t)}{\sqrt{2}} Q_\pi \left(k^\mu \frac{q \cdot \epsilon}{q \cdot k} - \epsilon^\mu \right) \\
&\quad \bar{u}(p_e, \lambda_e) \gamma_\mu (1 - \gamma_5) v(p_\nu, \lambda_\nu),
\end{aligned} \tag{20}$$

which coincides with formula (14) of Ref. [17] though their form are different. If only the first term of our formula (20) would be taken,

$$\begin{aligned}
M_{I'}^0 &= \frac{G_F V_{us} F_{K\pi}(t)}{\sqrt{2}} \bar{u}(p_e, \lambda_e) \left[\left(Q_e \frac{p_e \cdot \epsilon}{p_e \cdot k} + Q_\pi \frac{q \cdot \epsilon}{q \cdot k} \right) \right. \\
&\quad \left. + Q_e \frac{\not{\epsilon} \not{k}}{2p_e \cdot k} \right] (2 \not{q} + m_e) (1 - \gamma_5) v(p_\nu, \lambda_\nu).
\end{aligned} \tag{21}$$

Then the resulting gauge invariant formula (21) is not anymore consistent with the leading logarithm approximation for a photon emission collinear with the π^\pm . On the other hand, for the K^0 decay there is no collinear enhancement of photon emission along the π^\pm direction because it is not ultrarelativistic. This is why the inconsistency has no practical consequences for K^0 decay but may be of importance for the case of B_{l3} decays. The case would be then quite similar to the one of Ref. [11] (formulas (11) and (13) there) and is also rather simple to fix without return to the complete formula (20). Improved in that respect formula (21) would read:

$$\begin{aligned}
M_{II'}^0 &= \frac{G_F V_{us} F_{K\pi}(t)}{\sqrt{2}} \bar{u}(p_e, \lambda_e) \left[\left(Q_e \frac{p_e \cdot \epsilon}{p_e \cdot k} + Q_\pi \frac{q \cdot \epsilon}{q \cdot k} \right) \right. \\
&\quad \left(2 \left(\not{q} + \not{k} \frac{p_e \cdot k}{q \cdot k + p_e \cdot k} \right) + m_e \right) \\
&\quad \left. + Q_e \frac{\not{\epsilon} \not{k}}{2 p_e \cdot k} (2 \not{q} + m_e) \right] (1 - \gamma_5) v(p_\nu, \lambda_\nu). \tag{22}
\end{aligned}$$

We investigate it, as another option for bremsstrahlung matrix element in neutral K_{l3} decays.

Our formula (20) can be re-written also as a sum of $M_{II'}^0$ and $M_{II'}^0$:

$$\begin{aligned}
M_0 &= M_{II'}^0 + M_{II'}^0, \\
M_{II'}^0 &= 2 \frac{G_F V_{us} F_{K\pi}(t)}{\sqrt{2}} \left(\frac{k^\mu}{q \cdot k + p_e \cdot k} (Q_\pi q \cdot \epsilon + Q_e p_e \cdot \epsilon) \right. \\
&\quad \left. - Q_\pi \epsilon^\mu \right) \bar{u}(p_e, \lambda_e) \gamma_\mu (1 - \gamma_5) v(p_\nu, \lambda_\nu), \tag{23}
\end{aligned}$$

where $M_{II'}$ is free of singularities.

3 Differential decay probability.

As the spin states of the K_{l3} decay products are not measurable, we concentrate on differential distributions obtained from amplitudes squared and summing over lepton spin states.

3.1 Born and real emissions

Let us explore squares of amplitudes given by eqs. (12, 13). We use the following notations:

$$S = 2 p_e \cdot p_\nu, T = 2 q \cdot p_e, U = 2 q \cdot p_\nu. \tag{24}$$

The Born level expression for the charged K decay reads:

$$\begin{aligned}
\sum_{\text{Spin}} |M_{\text{Born}}^c|^2 &= \frac{G_F^2 |V_{us}|^2 F_{K\pi}^2(t)}{4} 32 \\
&\left[q \cdot p_\nu (2q \cdot p_e + m_e^2) - \left(m_\pi^2 - \frac{m_e^2}{4} \right) p_\nu \cdot p_e \right] \\
&= \frac{G_F^2 |V_{us}|^2 F_{K\pi}^2(t)}{4} 16 \\
&\left[U (T + m_e^2) - \left(m_\pi^2 - \frac{m_e^2}{4} \right) S \right]. \tag{25}
\end{aligned}$$

For the bremsstrahlung case, the square of the amplitude is given by

$$\begin{aligned}
\sum_{\text{Spin}} |M^c|^2 &= \sum_{\text{Spin}} |M_{I'}^c|^2 + \sum_{\text{Spin}} |M_{II'}^c|^2 \\
&\quad + 2 \sum_{\text{Spin}} M_{I'}^c M_{II'}^{c*}, \tag{26}
\end{aligned}$$

where

$$\begin{aligned}
\sum_{\text{Spin}} |M_{I'}^c|^2 &= 32 \sum_{i=1,2} \left(Q_e \frac{p_e \cdot \epsilon_i}{p_e \cdot k} - Q_K \frac{p \cdot \epsilon_i}{p \cdot k} \right)^2 \\
&\quad \frac{G_F^2 |V_{us}|^2 F_{K\pi}^2(t)}{4} \left[q \cdot p_\nu (2q \cdot p_e + m_e^2) \right. \\
&\quad \left. - \left(m_\pi^2 - \frac{m_e^2}{4} \right) p_\nu \cdot p_e \right], \tag{27}
\end{aligned}$$

$$\begin{aligned}
\sum_{\text{Spin}} |M_{II'}^c|^2 &= \frac{-16Q_e^2}{p_e \cdot k} \sum_{i=1,2} (\epsilon_i \cdot \epsilon_i) \frac{G_F^2 |V_{us}|^2 F_{K\pi}^2(t)}{4} \\
&\quad \left[2q \cdot p_\nu q \cdot k - \left(m_\pi^2 - \frac{m_e^2}{4} \right) p_\nu \cdot k \right] \tag{28}
\end{aligned}$$

$$\begin{aligned}
2 \sum_{\text{Spin}} M_{I'}^c M_{II'}^{c*} &= 32 \frac{G_F^2 |V_{us}|^2 F_{K\pi}^2(t)}{4} \\
&\left[\sum_{i=1,2} Q_e \frac{p_e \cdot \epsilon_i}{p_e \cdot k} \left(Q_e \frac{p_e \cdot \epsilon_i}{p_e \cdot k} - Q_K \frac{p \cdot \epsilon_i}{p \cdot k} \right) \right. \\
&\quad \left(2q \cdot p_\nu q \cdot k - \left(m_\pi^2 - \frac{m_e^2}{4} \right) p_\nu \cdot k \right) \\
&\quad - \sum_{i=1,2} Q_e \left(Q_e \frac{p_e \cdot \epsilon_i}{p_e \cdot k} - Q_K \frac{p \cdot \epsilon_i}{p \cdot k} \right) \\
&\quad \left. \left(2q \cdot p_\nu q \cdot \epsilon_i - \left(m_\pi^2 - \frac{m_e^2}{4} \right) p_\nu \cdot \epsilon_i \right) \right].
\end{aligned} \tag{29}$$

Here ϵ_1, ϵ_2 are two orthogonal photon polarization vectors. As expected $\sum |M_{I'}^c|^2$ consists of a Born-like expression multiplied by an eikonal factor. The second and third terms, $\sum |M_{II'}^c|^2$ and $2 \sum M_{I'}^c M_{II'}^{c*}$, are free of soft singularities.

Formulae for charged K^- decay and neutral $K^0 \rightarrow \pi^+ e^- \bar{\nu}_e$ are similar. Obtained from formula (14)

$$\sum_{\text{Spin}} |M_{\text{Born}}^0|^2 = 2 \times \sum_{\text{Spin}} |M_{\text{Born}}^c|^2 \tag{30}$$

differs from the Born contribution of charged K decay by a factor of 2. For the bremsstrahlung case, the amplitude squared can be again separated into parts. The first one consists³ of the squared formula (22), which reads:

$$\begin{aligned}
\sum_{\text{Spin}} |M_{I''}^0|^2 &= 2 \times \sum_{\text{Spin}} |M^c|^2 \\
&\quad Q_{K \rightarrow -Q\pi, \frac{p \cdot \epsilon_i}{p \cdot k} \rightarrow \frac{q \cdot \epsilon_i}{q \cdot k}} \\
&+ 32 \frac{G_F^2 |V_{us}|^2 F_{K\pi}^2(t)}{2} \frac{p_e \cdot k}{q \cdot k + p_e \cdot k} \times \\
&\quad \left[\sum_{i=1,2} \left(Q_e \frac{p_e \cdot \epsilon_i}{p_e \cdot k} + Q_\pi \frac{q \cdot \epsilon_i}{q \cdot k} \right)^2 (k \cdot p_\nu (2q \cdot p_e + m_e^2)) \right. \\
&\quad + 2 \left(q \cdot p_\nu + \frac{p_e \cdot k}{q \cdot k + p_e \cdot k} k \cdot p_\nu \right) k \cdot p_e - 2q \cdot k p_\nu \cdot p_e \\
&\quad + \sum_{i=1,2} 2Q_e \left(Q_e \frac{p_e \cdot \epsilon_i}{p_e \cdot k} + Q_\pi \frac{q \cdot \epsilon_i}{q \cdot k} \right) \\
&\quad \left. (p_\nu \cdot \epsilon_i q \cdot k - q \cdot \epsilon_i p_\nu \cdot k) \right].
\end{aligned} \tag{32}$$

³First term can be obtained from formula (27,28,29) with the help of the change of variables

$$Q_K \rightarrow -Q_\pi, \quad \frac{p \cdot \epsilon_i}{p \cdot k} \rightarrow \frac{q \cdot \epsilon_i}{q \cdot k}. \tag{31}$$

The second part, contributing to the squared amplitude for neutral K decay, consists of the squared formula (23) and its interference with formula (22). We do not write explicitly this expression here, as it is rather lengthy, and is numerically small.

3.2 Virtual corrections

Virtual corrections to K_{l3} decays can be found eg. in Ref. [17], they are of lesser importance than the real ones and we do not recall them here. The present work is devoted to the discussion of real emission corrections, which are experimental condition dependent. Virtual corrections have to be divided into two parts. One part is large, but adds up to zero with real emissions in total rate thanks to Kinoshita-Lee-Nauenberg theorem. This part is taken into account by the PHOTOS Monte Carlo code. The other part has to be included in the form-factor and incorporated to the Born level matrix element. For this purpose, real emission amplitude squared need to be integrated over photon momentum to control the sum rule to the level of complete first order. This can be performed in an approximate way⁴ (as in Ref. [19]) or in an exact manner, following phase space parametrization as used in PHOTOS. Integration (analytic or numerical) need to be performed. This solution has to be adopted, once experimental precision approaches $\frac{\alpha}{\pi}$ precision level. Still another type of solution, non exploiting the sum rule of Konoshita-Lee-Nauenberg can be useful. We mention such possibility in footnote 5.

4 Monte Carlo Simulation

We use the TAUOLA [20] code to generate Born level K decay samples. For practical reasons this generator is suitable for our purpose once the τ decay matrix element is replaced with the one of the K_{l3} decay, and appropriate adjustment of masses and particle identifiers are performed. Semileptonic decays of τ 's are suitable for such adaptation⁵. Another advantage is that we can then guarantee full control of parameters used in our Born level generator and in matrix element of PHOTOS correcting weights.

We gain, because PHOTOS is ready to use with TAUOLA. The two programs share technical elements. This is convenient when non-factorizable parts of matrix elements are installed. The interface to HEPEVT event record of the two programs offers an easy access to our testing tool MC-TESTER [21, 22]. The prepared plots are then compatible with our previous studies. From the user point of view, numerical results collected for this paper, and available also in graphic form from the web-page [23], can be of interest for benchmarking K decay generators independently, whether they are coded in FORTRAN or in C++.

⁴But then, no gain beyond Konoshita-Lee-Nauenberg can be achieved. In K_{e3} decay there is no Coulomb effect.

⁵TAUOLA semileptonic decay channel offer an alternative crude phase space generator for radiative corrections, which may become useful in the future, especially if complete virtual corrections are to be included and studied.

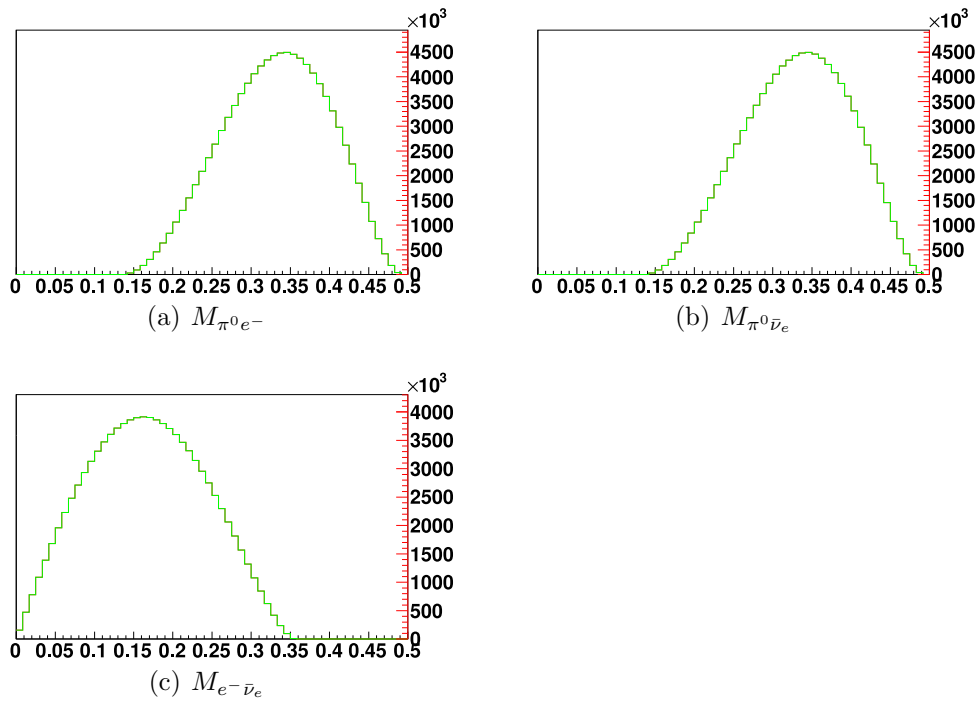


Figure 2: Distributions of invariant masses, in GeV (GeV/c^2 , $c = 1$) units, constructed from the products of the decay $K^- \rightarrow \pi^0 e^- \bar{\nu}_e$, at Born level. As in [24] $V_{us} = 0.2252$ is used, we take however $F_{K\pi}(t) = 1$. This is an acceptable approximation for our purposes and consistent with Ref.[17].

The squares of Born level amplitudes (25) for decays $K^- \rightarrow \pi^0 e^- \bar{\nu}_e$, and $K^0 \rightarrow \pi^+ e^- \bar{\nu}_e$ are rather easy to implement into TAUOLA. The numerical results, as histograms of invariant masses constructed from pairs of final state decay products, are shown in Fig. 2. We have compared these results with the one of Ref. [25] and reasonable agreement was found. This comparison is sufficient for tests, because the matrix element is rather simple and TAUOLA itself is well tested. Note that detector acceptance effects were included in Ref. [25], therefore the corresponding figures do not coincide in all details with our Fig. 2.

5 Numerical results

In all tests presented in this paper we use samples of 100 million events. We refer to standard PHOTOS whenever we use its publicly available FORTRAN version 2.15, or any other version which yields equivalent results. In particular, identical results are available (as default option) from the C++ PHOTOS [26], version 3.0 or higher. One of the goals of the present work is to provide a systematic error for these widely used versions.

As a first step, we perform a technical test. For the decay of charged K we have compared results of the standard PHOTOS with the PHOTOS version of [10]. It was the first version where the multiphoton phase space generation for final state of a single charged (and scalar) particle was exact, which was provided with the help of explicit phase space Jacobians. It is publicly available starting from PHOTOS++, version 3.3. We could see that the numerical effect is small. As expected, the difference is below 0.05 % if calculated with respect to the total rate. We obtained differences at the level of 10 % in regions of phase space contributing at the level of 10^{-4} to the total rate.

In a second step, we have checked the contribution from collinear photon emission region. To this end we have selected only those events, used in the previous comparison, where the photon-electron pair invariant mass was at most 0.01 of their energies product (taken in the rest frame of K). We obtained perfect agreement, with no statistically significant differences.

Only then, results presented in our article were prepared. Throughout the paper, we use our testing program MC-TESTER [21, 22]. The two colored (grey) lines correspond to the compared generation samples⁶. To define the boundary of the real emission phase space we use the photon energy in the rest frame of the decaying kaon: it is set at 0.005 of the decaying kaon mass.

We have repeated the same comparison as discussed previously but when the complete scalar QED matrix element is installed. As we can see from Fig. 3 the numerical effect of the Matrix Element and exact phase space implementation is rather small, visible only at the ends of the spectra (contributing at the level of 10^{-3} to the total rate) where relative

⁶ The distributions of Lorentz invariants constructed from outgoing particles are shown. Additional information is available on plots of the web-page [23]. The SDP (shape difference parameter) obtained from MC-TESTER represents an exclusive surface (normalized to unity) under the green and red distributions. The statistical error (calculated in a rather simplified way) is subtracted from this difference. The black line is the ratio of the distributions.

differences are sizable. There, matrix element effects are rather substantial and should be kept in mind in some contexts, e.g. for generating background to other decays.

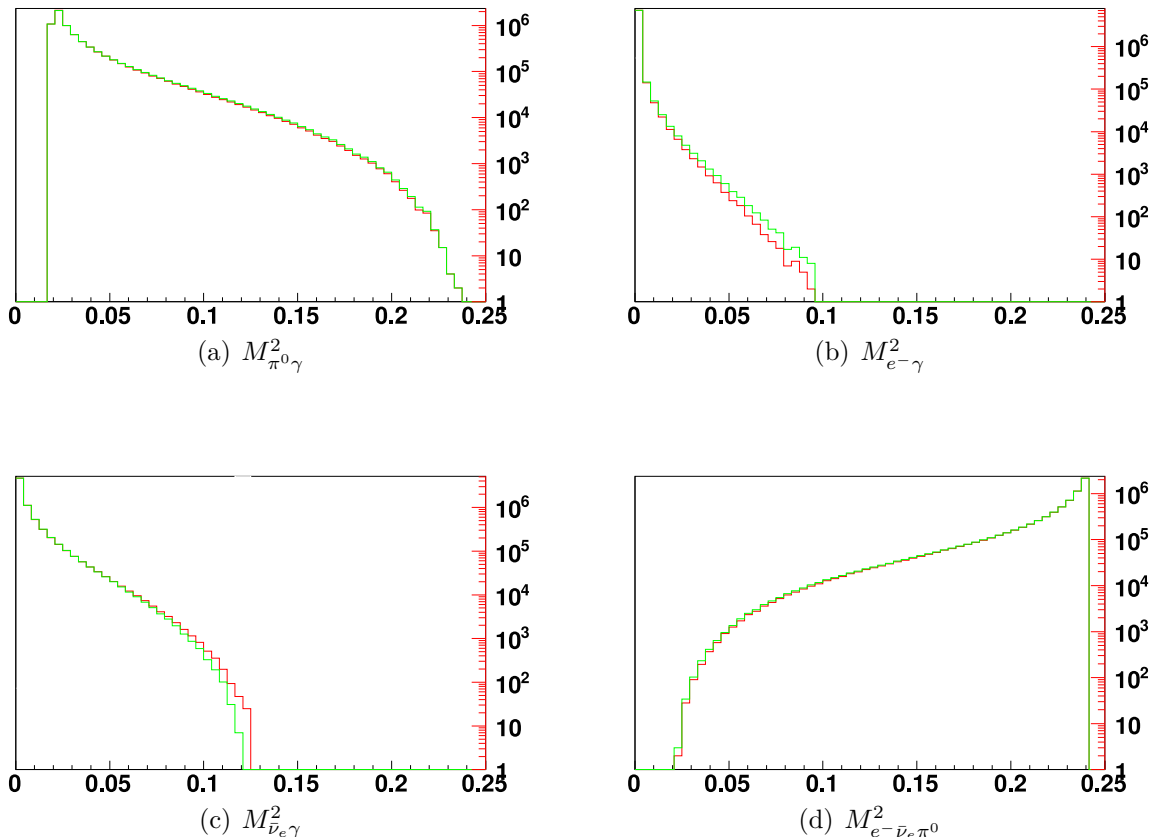


Figure 3: Distributions of scalar Lorentz invariants, in GeV^2 (GeV^2/c^4 , $c = 1$) units, constructed from the decay products in $K^- \rightarrow \pi^0 e^- \bar{\nu}_e$ channel. The most sensitive invariants to photon energy are plotted. The red (darker grey) line is standard PHOTOS, the green is with exact Matrix Element. The fraction of accepted bremsstrahlung events is (7.371 ± 0.0027) % in standard PHOTOS run and (7.4127 ± 0.0027) % when the matrix element is used.

For the case of $K^- \rightarrow \pi^0 \mu^- \bar{\nu}_\mu$, logarithmic corrections are of course much smaller. That is why non leading terms contribute to photon spectra in a relatively larger manner, and seemingly much larger effects can be seen in Fig. 4 than in Fig. 3. Nonetheless it is not more significant numerically. Only 0.45 % of events enter the plots for the muonic channel; twenty times less than in the electron case. We can conclude that standard PHOTOS works sufficiently well for the $K^- \rightarrow \pi^0 \mu^- \bar{\nu}_\mu$ decay, if one is interested in 0.2 % precision limits.

The $K^0 \rightarrow \pi^+ l^- \bar{\nu}_l$ case is technically more interesting as two kinematical branches are present in the crude level phase space generator.

In Fig. 5 we compare standard PHOTOS with a version where the scalar QED matrix

element is installed. The approximation in the phase space is still present. Only in Fig. 6 we use single channel presampler for the phase space generation and the phase space is exact. The effect of phase space Jacobian approximation is rather small.

By comparing Figs. 7 and 6 we can see that the standard PHOTOS is much closer to the result of scalar QED matrix element than to one of (21). The bulk of the difference is due to the non-compatibility of formula (21) with collinear logarithms due to emission from charged pion (we can see it by comparing Fig. 8). This is of course beyond the framework of approximation at use, but it is nonetheless of some interest, to understand the origin of the residual differences between possible options for the matrix element and how to fix it in gauge invariant way, but without study of the whole matrix element.

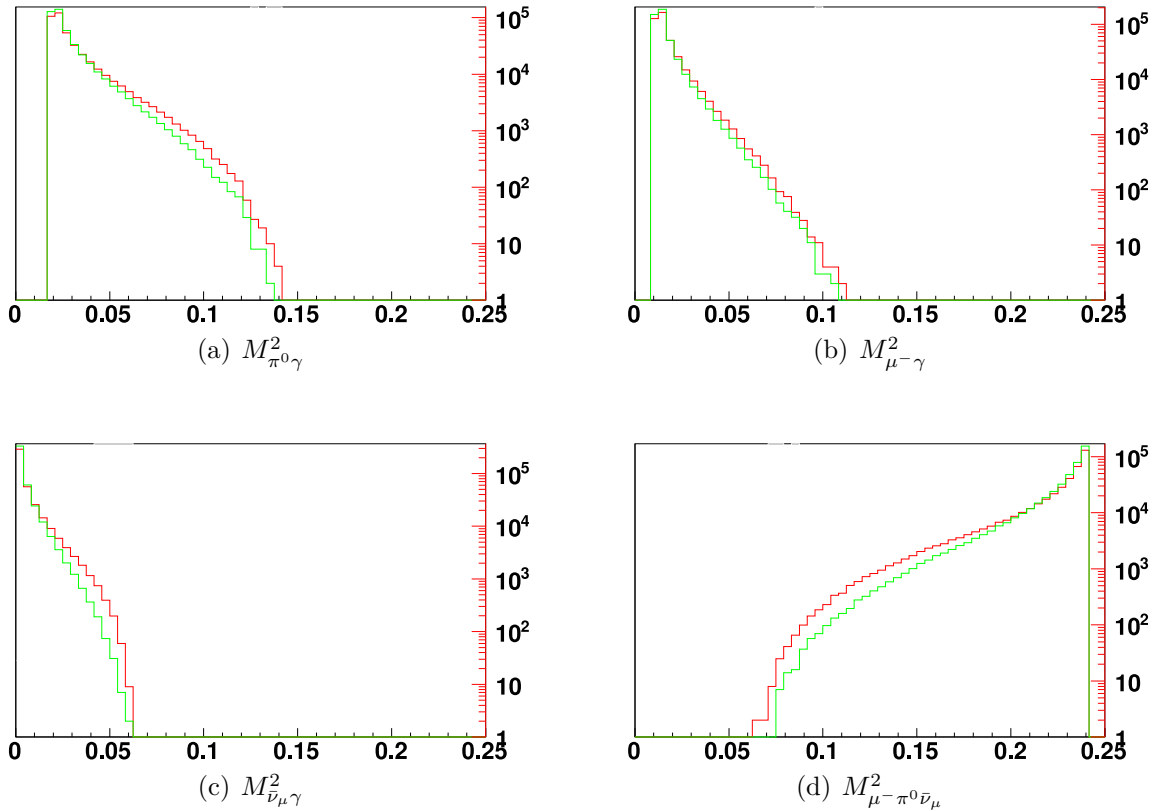


Figure 4: Distributions of scalar Lorentz invariants, in GeV^2 (GeV^2/c^4 , $c = 1$) units, constructed from the decay products in $K^- \rightarrow \pi^0 \mu^- \bar{\nu}_\mu$ channel. Invariants most sensitive to photon energy are shown. The red (darker grey) line is standard PHOTOS, the green is with exact Matrix Element. One could conclude that the effect of matrix element introduction is not small in this case. However, only a small fraction of events enter this plot (0.4113 ± 0.0006) % for standard PHOTOS and (0.4445 ± 0.0007) % for the case with matrix element. The difference is well below 0.1 % when compared to the total rate. The two distributions coincide in the soft photon region.

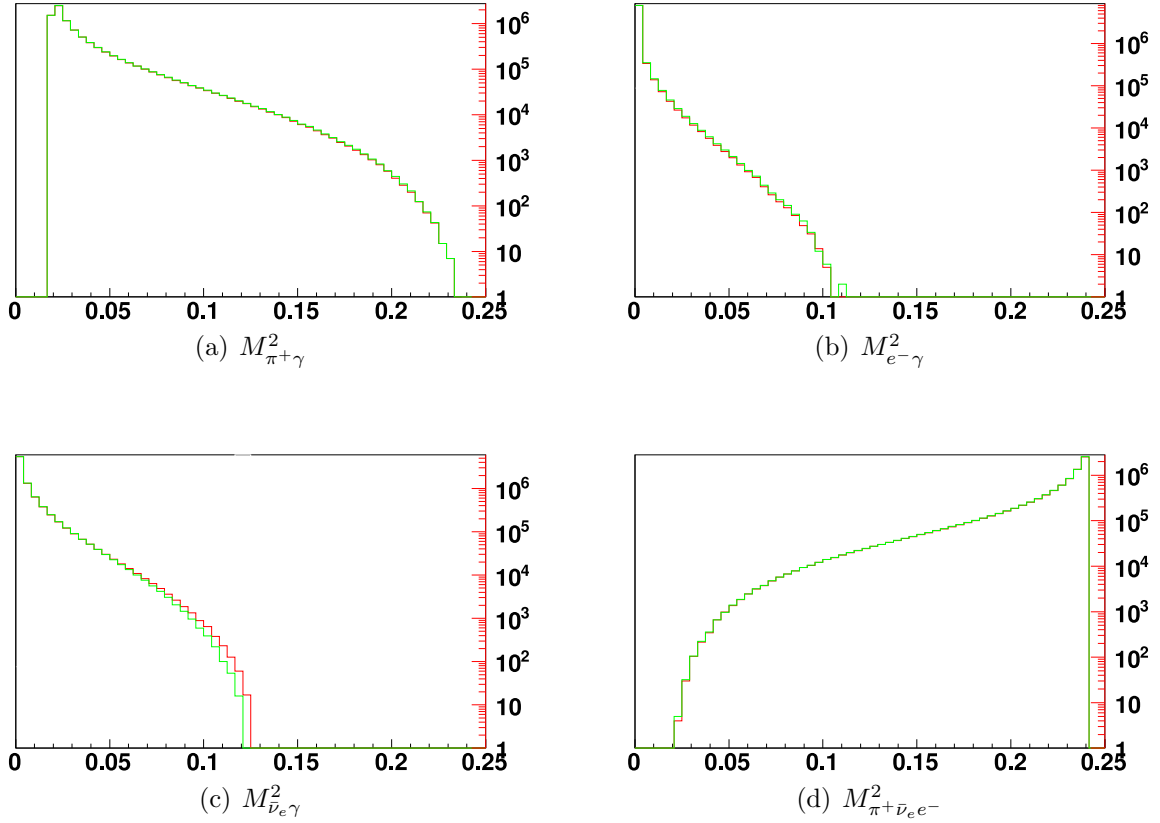


Figure 5: Distributions of scalar Lorentz invariants, in GeV^2 (GeV^2/c^4 , $c = 1$) units, constructed from the decay products in $K^0 \rightarrow \pi^+ e^- \bar{\nu}_e$ channel. The most sensitive invariants to photon energy are plotted. Two kinematical branches are used, thus the phase space is not exact. The red (darker grey) line is standard PHOTOS, the green is with exact Matrix Element. The fraction of accepted bremsstrahlung events is $(8.6398 \pm 0.0029) \%$ in standard PHOTOS run and $(8.6913 \pm 0.0029) \%$ when the matrix element is used.

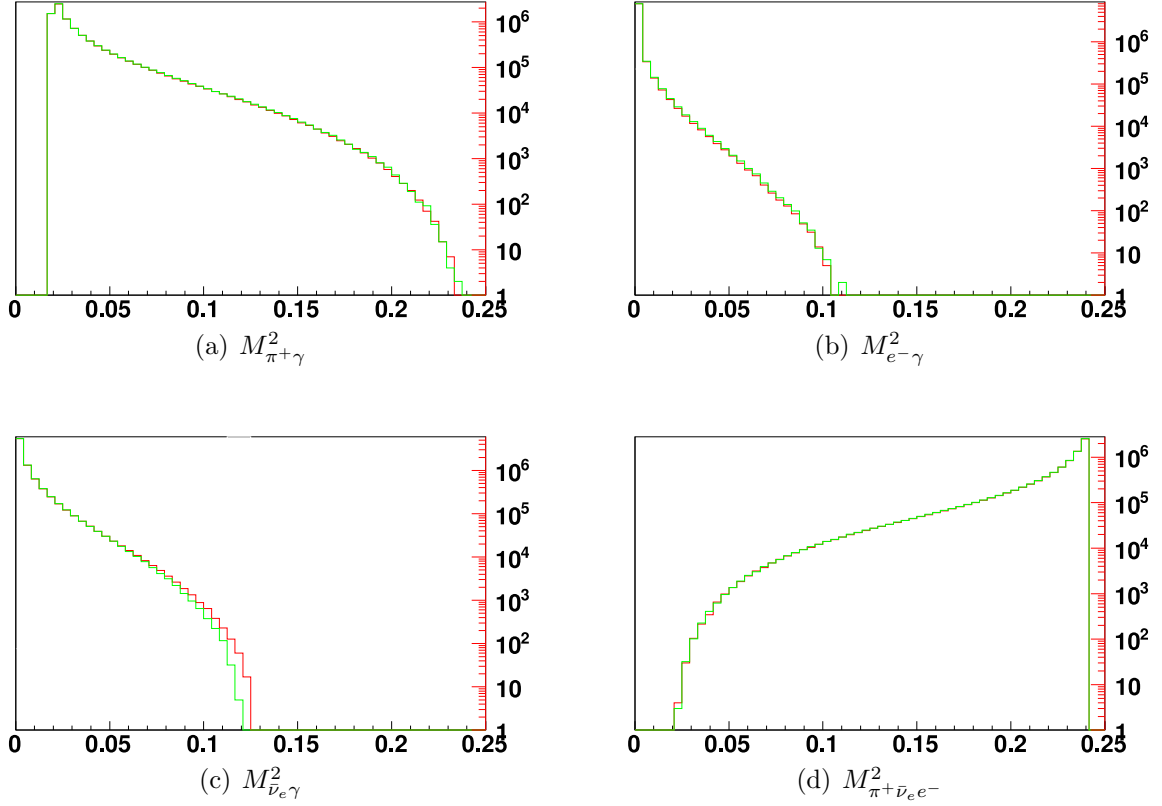


Figure 6: Distributions of scalar Lorentz invariants, in GeV^2 (GeV^2/c^4 , $c = 1$) units, constructed from the decay products in $K^0 \rightarrow \pi^+ e^- \bar{\nu}_e$ channel. The most sensitive invariants to photon energy are plotted. Single kinematical branch is used, thus the phase space is exact. The red (darker grey) line is standard PHOTOS, the green is with exact Matrix Element. The fraction of accepted bremsstrahlung events is $(8.6398 \pm 0.0029) \%$ in standard PHOTOS run and $(8.6958 \pm 0.0029) \%$ when the matrix element is used.

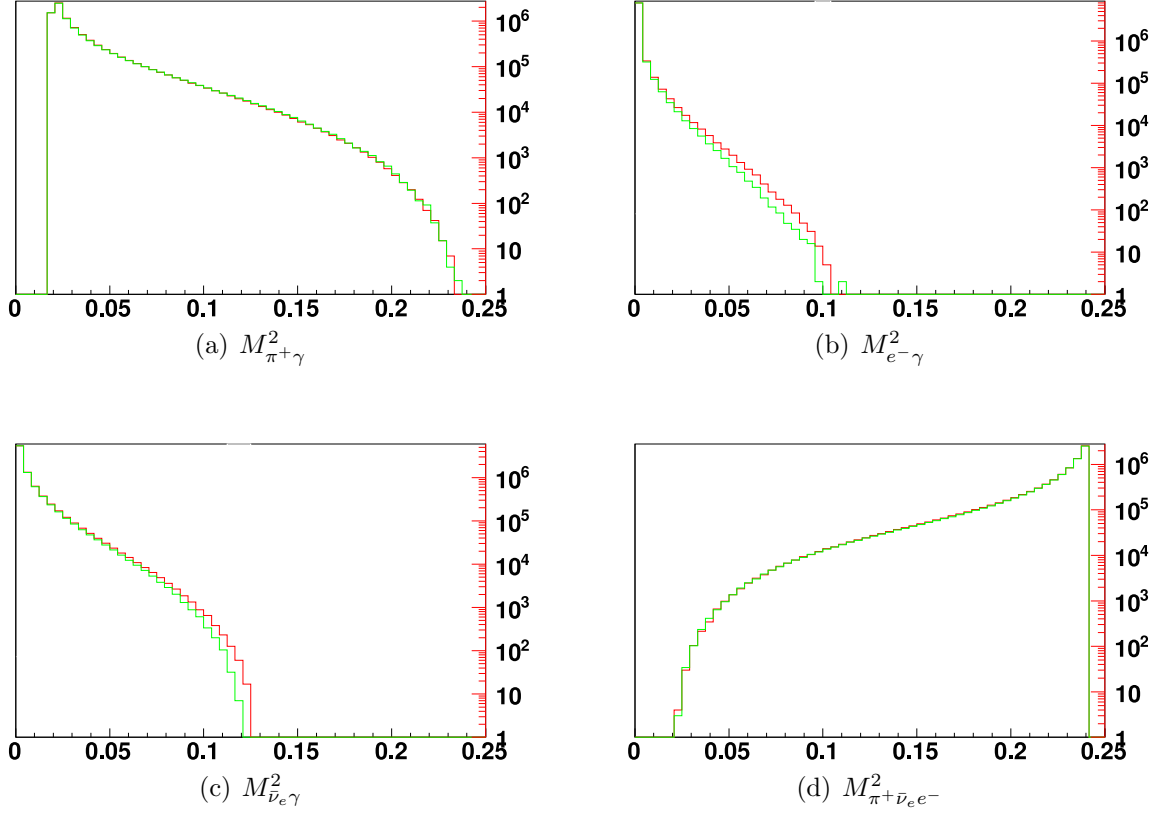


Figure 7: Distributions of scalar Lorentz invariants, in GeV^2 (GeV^2/c^4 , $c = 1$) units, constructed from the decay products in $K^0 \rightarrow \pi^+ e^- \bar{\nu}_e$ channel. The most sensitive invariants to photon energy are plotted. Single kinematical branch is used, thus the phase space is exact. The red (darker grey) line is standard PHOTOS, the green is with exact Matrix Element. The fraction of accepted bremsstrahlung events is $(8.6398 \pm 0.0029) \%$ in standard PHOTOS run and $(8.5235 \pm 0.0029) \%$ when matrix element (21) is used.

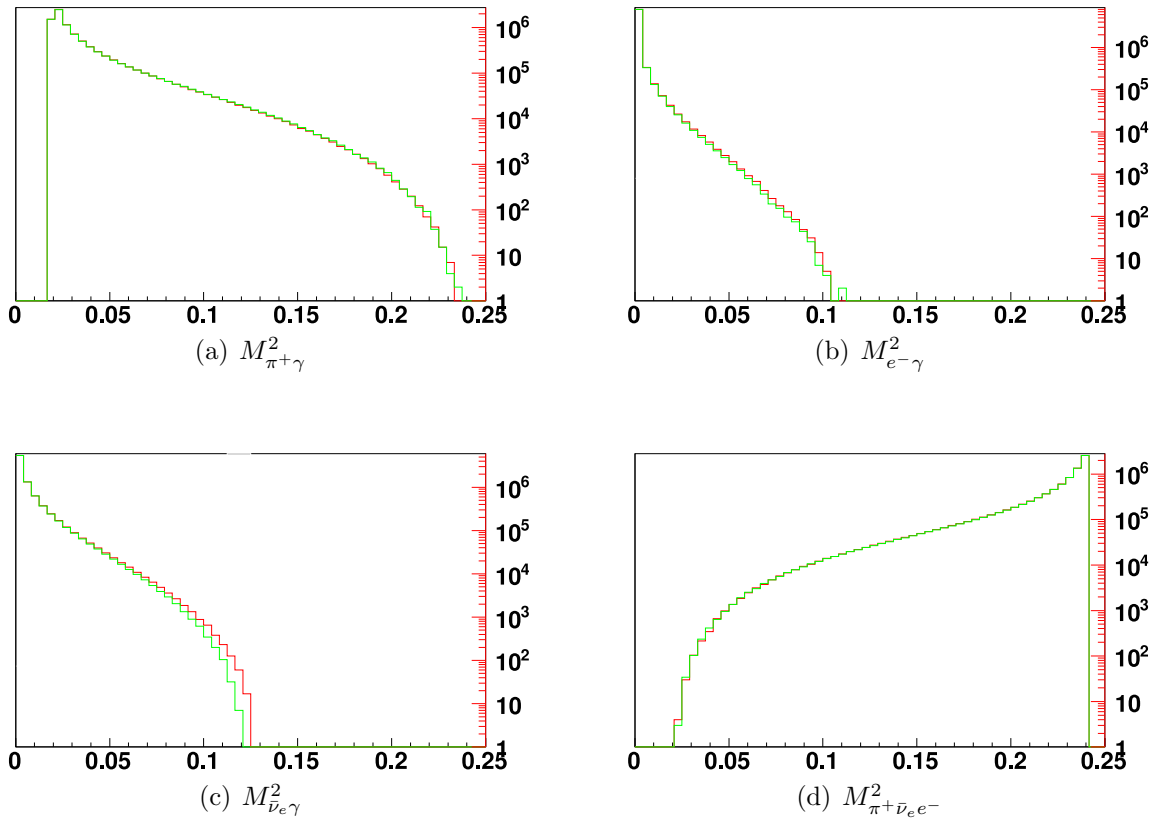


Figure 8: Distributions of scalar Lorentz invariants, in GeV^2 (GeV^2/c^4 , $c = 1$) units, constructed from the decay products in $K^0 \rightarrow \pi^+ e^- \bar{\nu}_e$ channel. The most sensitive invariants to photon energy are plotted. Single kinematical branch is used, thus the phase space is exact. The red (darker grey) line is standard PHOTOS, the green is with exact Matrix Element. The fraction of accepted bremsstrahlung events is $(8.6398 \pm 0.0029) \%$ in standard PHOTOS run and $(8.5928 \pm 0.0029) \%$ when matrix element (21) with improvement of formula (22) is used.

6 Summary

In this study we have adopted the matrix element of [17] for the emission kernel of PHOTOS Monte Carlo [7, 8, 10]. We have investigated semileptonic decays of kaons into π and lepton neutrino pair. After modification for these channels, PHOTOS features exact matrix element (three options) and exact (or default) phase space. We have evaluated the numerical size of the missing terms in publicly available version of PHOTOS. The difference is of the order of 0.2 %, thus rather small, except for the distribution of lepton photon pair invariant mass spectrum, where the difference is sizable at the high end of the spectrum in case of K^0 decay.

On the technical side, we have also checked the algorithm. We have compared the case when the pre-sampler is active for possible collinear singularity along lepton only (for which the phase space is exact and phase space Jacobians are explicit), and the case when both pre-samples for singularities along lepton and charged π directions are active. Such studies for more than 2 body decays were not documented until now. We found the differences to be below 0.05 %. Our work is supplemented with a larger set of figures, which are available from the web-page [23].

We conclude that for PHOTOS version 2.15 or higher, and for K_{l3} decays, the precision level with respect to matrix elements based simulation is 0.2% or better. This conclusion extends naturally to the case of multiple photon emission. We have identified the factorization properties of the matrix element, which were the reason why the differences were small. On the other hand, our error estimation is not complete. It does not include any discussion of uncertainty in the matrix elements due to assumptions of the models used for their calculation. Also, non leading effects of virtual corrections, which are expected to contribute at a similar 0.2 % level, are not discussed. They depend on the details of hadronic interactions and can not be tackled in discussion of bremsstrahlung only.

Acknowledgements

We would like to thank Tomasz Przedzinski for help in obtaining the numerical results presented in this paper and Brigitte Bloch-Devauux for help in improving the paper readability. We would like to thank referee of EPJC for identifying an error in our handling of formula (14) of Ref. [17].

References

- [1] M. Antonelli, V. Cirigliano, G. Isidori, F. Mescia, M. Moulson, *et al.*, *Eur.Phys.J.* **C69** (2010) 399.
- [2] S. Actis *et al.*, *Eur. Phys. J.* **C66** (2010) 585.
- [3] D. R. Yennie, S. Frautschi, and H. Suura, *Ann. Phys. (NY)* **13** (1961) 379.
- [4] S. Jadach and B. F. L. Ward, *Phys. Rev.* **D38** (1988) 2897.

- [5] S. Jadach, Z. Wąs, and B. F. L. Ward, *Comput. Phys. Commun.* **130** (2000) 260, Up to date source available from <http://home.cern.ch/jadach/>.
- [6] E. Barberio, B. van Eijk, and Z. Wąs, *Comput. Phys. Commun.* **66** (1991) 115.
- [7] E. Barberio and Z. Wąs, *Comput. Phys. Commun.* **79** (1994) 291.
- [8] P. Golonka and Z. Was, *Eur. Phys. J.* **C45** (2006) 97.
- [9] P. Golonka and Z. Was, *Eur. Phys. J.* **C50** (2007) 53.
- [10] G. Nanava and Z. Was, *Eur. Phys. J.* **C51** (2007) 569.
- [11] G. Nanava, Q. Xu, and Z. Was, *Eur.Phys.J.* **C70** (2010) 673.
- [12] N. Davidson, G. Nanava, T. Przedzinski, E. Richter-Was and Z. Was, *Comput. Phys. Commun.* **183** (2012) 821.
- [13] M. E. Peskin and D. V. Schroeder, *An Introduction to Quantum Field Theory*, Westview Press, 1995.
- [14] S. Weinberg, *Physica* **A96** (1979) 327, Festschrift honoring Julian Schwinger on his 60th birthday.
- [15] J. Gasser and H. Leutwyler, *Annals Phys.* **158** (1984) 142.
- [16] H. Leutwyler, *Annals Phys.* **235** (1994) 165.
- [17] V. Cirigliano, M. Giannotti, and H. Neufeld, *JHEP* **0811** (2008) 006.
- [18] V. Cirigliano, *PoS KAON* (2008) 007.
- [19] Y. Bystritskiy, S. Gevorkyan, and E. Kuraev, *Eur.Phys.J.* **C64** (2009) 47.
- [20] M. Jezabek, Z. Wąs, S. Jadach, and J. H. Kühn, *Comput. Phys. Commun.* **70** (1992) 69.
- [21] P. Golonka, T. Pierzchala, and Z. Was, *Comput. Phys. Commun.* **157** (2004) 39.
- [22] N. Davidson, P. Golonka, T. Przedzinski, and Z. Was, *Comput. Phys. Commun.* **182** (2011) 779.
- [23] Projects 2011/12 on <http://wasm.web.cern.ch/wasm/> or <http://hibiscus.if.uj.edu.pl/~przedzinski/Kl3/>.
- [24] Particle Data Group Collaboration, K. Nakamura *et al.*, *J. Phys.* **G37** (2010) 075021.
- [25] NA48/2 Collaboration, J. R. Batley *et al.*, *Eur. Phys. J.* **C50** (2007) 329.
- [26] N. Davidson, T. Przedzinski and Z. Was, “PHOTOS Interface in C++: Technical and Physics Documentation,” arXiv:1011.0937 [hep-ph].